

A Satellite Mobile Communication System Based on Band-Limited Quasi-Synchronous Code Division Multiple Access (BLQS-CDMA)

R. De Gaudenzi, C. Elia, R. Viola

European Space Agency (ESA)
European Space Research and Technology Centre
RF System Division
P.O. Box 200, 2200 AG Noordwijk The Netherlands

Abstract

In this paper we discuss a new approach to code division multiple access applied to mobile system for voice (and data) services based on Band Limited Quasi Synchronous CDMA (BLQS-CDMA). The system requires users to be chip synchronized to reduce the contribution of self-interference and to make use of voice activation in order to increase the satellite power efficiency.

In order to achieve spectral efficiency, Nyquist chip pulse shaping is utilized with no detection performance impairment.

The synchronization problems are solved in the forward link by distributing a master code, whereas carrier forced activation and closed loop control techniques have been adopted in the return link.

System performance sensitivity to non-linear amplification and timing/frequency synchronization errors is analyzed.

1 Introduction

As technology progresses offering services for mobile users with higher satellite EIRP per channel, the bandwidth limitations are more and more the key problem of high capacity services. This is especially true for L-band, where currently mobile services are supposed to operate.

In this contest an efficient use of the available spectrum, optimizing the satellite access system, is of capital importance. A selected access system has also to account for the difficult environment characterizing land mobile communications, where users are frequently subjected to deep shadowing and multipath conditions.

ESA is now embarking in activities centered around deployment of a new satellite system dedicated to Europe Mobile Service (EMS). This satellite will provide business voice/data services in the framework of private land mobile networks (PMR).

EMS will have an initial development phase based on a global beam coverage of Europe and subsequently it will be upgraded with a multi-beam antenna system.

In this framework studies to optimize the access scheme and the network are presently carried out. Code division multiple access is one of the candidates.

Considering the hostile environmental conditions, CDMA was always regarded as an attractive but inefficient access scheme for satellite mobile services. Techniques for increasing the CDMA efficiency were recently introduced [3]. The key idea is to reduce the voice duty cycle by employing carrier voice activation which reduces the average number of contemporary users. Moreover CDMA allows frequency reuse by polarization discrimination, being the cross-polarization effects reduced by the code diversity. In a multi-beam environment further advantages have been predicted in ref. [3].

A more substantial advantage which has never been exploited in traditional asynchronous CDMA systems is the drastic reduction of self-noise interference when synchronous CDMA is used [6]. Synchronous CDMA means that every user is using a common clock reference and on this basis the signature sequence transmission is aligned.

The attractive performances of S-CDMA described in ref. [6], refers to the unfiltered case. In practical system spectral compactness is of primary relevance and shall be achieved with minor end-to-end performance degradation.

In the following we show how the use of Nyquist chip pulse shaping allows to maintain the same performances of the unfiltered case.

It is also clear that perfect carrier and clock synchronization among different users can not be kept especially in the mobile environment [7]. Due to the user carriers incoherency and relative timing jitter affecting different signals, the system is named band limited quasi-synchronous CDMA (BLQS-CDMA).

The use of synchronization yields to simple implementation of voice activation in the forward and return link, thus avoiding all problems connected with fast code acquisition and tracking.

Voice activation is in fact important also in a synchronized system providing power savings and further reduction of the self-interference.

2 System Overview

Our reference system is a private mobile network composed of a transparent satellite transponder, a distributed feeder link

and a large number of mobile users distributed over a vast geographical area (see Fig. 1). The access system is CDMA both in forward and return link.

As depicted in Fig. 1, the system is composed by a network coordination station (NCS), a certain number of fixed earth stations (FES) connected with the ground network or directly placed at corporate user location. FES's provide two way voice/data communications with the mobile user terminals (MTs).

Each MT has the capability to transmit/ receive compressed digital voice, data, signalling information. A special code is reserved to the master station called *master code* (MC) [5], [6]. This code (not necessarily of the same type of user codes), is broadcasted to every MT and is used for frequency and time synchronization purposes. The signalling low data rate information is direct sequence spread by the MC and transmitted from the NCS in TDM fashion to the MT's

A master-to-user signal power ratio in the range of [5-10] dB can be set without significant loss of capacity. This is extremely beneficial for the network performances in case of shadowing. In fact, the mobile terminal drastically reduces traffic channel reacquisition time by increasing master channel availability. Moreover master signal level monitoring at MTs provides a tool for open loop power control.

To each mobile terminal two codes are assigned, one for the I ($c_p(t)$) and one for the Q channel ($c_q(t)$).

Return link synchronization is achieved through MT's time/frequency comparison with the master reference. MT's synchronization errors are detected at the FES, then coded and looped back to the corresponding MT's together with the useful information.

In the following paragraphs a description of the elements composing the system will be given, detailing the mechanisms generally described in this section.

3 System Description

3.1 Modulation Technique

The selected modulation scheme is basically a direct sequence QPSK with independent I and Q signature sequences. *Ad hoc* chip shaping, satisfying the Nyquist criterium, is employed in order to obtain a band-limited signal. This point is of major relevance because more traditional filtering approach can affect the S-CDMA small sensitivity to self-noise interference. The use of DS/QPSK with independent I-Q codes is essentially dictated by system robustness requirements to non ideal conditions (i.e. non-linear amplifier, non perfect synchronization etc.).

The simulated spectrum at the satellite transponder input and output for a reduced scale ($M=7$, roll-off=0.4) BLQS-CDMA is presented in Fig. 2 and 3. For sake of comparison Fig. 2 also reports the spectrum of the signal with rectangular shaping. As HPA output filter an elliptical filter with two sided bandwidth of 1.5 the chip rate and stop band attenuation of 40 dB has been used. Observe the compactness and absence of sidelobes for both input and output signal's spectrum.

3.2 Synchronization Considerations

Each FES synchronizes its signature sequence start epoch, clock and carrier frequency using the received MC. In order to keep start epoch alignment, each station compares the phase of its own signature sequence looped back by the satellite with the NCS master reference. Measured timing error will be used to correct possible drifts. A similar concept apply for the FES carrier frequency and code timing control.

Delay compensation in MT terminals is instead performed by the FES's in closed loop to keep the mobile terminal as simple as possible.

3.3 Network Coordination Station Description

The NCS is dealing with :

- network master reference broadcasting and signalling,
- dynamic signature sequence allocation to MT's.

To fulfill to the above mentioned tasks the NCS requires a dedicated communication link with the FES.

3.4 Fixed Earth Station Description

A FES schematic block diagram is given in Figure 4. The received signal after IF conditioning feeds a bank of spread spectrum demodulators differing only in the signature code used for signal despreading.

Two of them named *echo demodulator* and *master demodulator* / are dedicated to FES synchronization errors detection.

The demodulated signals enter the Central Processor Unit which performs all necessary baseband processing such as:

- baseband demodulated user signals routing,
- signalling messages decoding,
- FES synchronization to the master reference,
- MT's synchronization error detection and coding

The digital baseband signal to be transmitted to the mobile users is composed by a synchronized set of different signature codes.

The resulting SS IF signals with equal power and carrier frequency are combined and up-converted to the transmission frequency prior final amplification. Signature sequence timing and carrier frequency is controlled by the so called *timing/frequency control unit*.

3.5 Mobile Terminal Description

In Figure 5 a principle block diagram of the user terminal is presented.

The RF-Front End of the *j-th user* delivers the IF signal which contains all the DS/SS signals plus the master code.

The master code is acquired and tracked by the dedicated sub-systems depicted in Figure 5. The on-time master code replica is used for despreading the master data stream which is routed to the modem central processor. Time epoch and

clock information supplied by the master code tracking loop drive the user I and Q codes replica generator.

The analog vocal signal on the transmitter side is first compressed, and then convolutionally coded. The I and Q symbol streams are logically added to the respective codes and used for carrier PSK modulation.

The up-link signal switch is controlled by the speech activity detector which is intended to interrupt the transmission during speech pauses.

The demodulator is being developed using full DSP approach and will include FIR chip pulse shaping filter equally shared between the transmitter and receiver side in order to achieve signal band-limitation.

4 System Performance Evaluation

The key novelty of the system consists in the use of a synchronous multiple access. Therefore the user BER evaluation based on the average SNR [2], or on the Gaussian interference approximation [1], is not anymore directly applicable. In ref. [8] it has been shown the validity of Gaussian interference approximation upon appropriate second order moment derivation.

Detailed derivations for the probability of error for the synchronous and quasi-synchronous cases are reported in [6], [7] respectively.

It has been shown that for S-CDMA the probability of error for the j -th user is well approximated by:

$$P_e^j = \frac{1}{2} \left[Q \left(\sqrt{\frac{\frac{2E_b}{N_0}}{1 + V \mu_j^p \frac{(M-1)}{2G_p} \frac{E_b}{N_0}}} \right) + Q \left(\sqrt{\frac{\frac{2E_b}{N_0}}{1 + V \mu_j^q \frac{(M-1)}{2G_p} \frac{E_b}{N_0}}} \right) \right] \quad (1)$$

$$Q(x) = \frac{1}{\sqrt{2\pi}} \int_x^\infty \exp\left(-\frac{x^2}{2}\right) dx$$

where the factor μ_j^l named *quadratic average cross-correlation factor* is defined as

$$\mu_j^l = \frac{1}{(M-1)} \sum_{i=1, i \neq j}^M [C_{i,j}^l]^2$$

$$C_{i,j}^l = \sum_{k=1}^N c_{k,i}^l c_{k,j}^l \quad l = p, q \quad (2)$$

where M is the number of users, T_b is the data bit duration, T_c is the chip duration, E_b/N_0 is the energy per bit to thermal noise density ratio, $G_p = T_b/T_c$, $c_{k,i}^{p,q}$ is the k -th chip of the i -th p, q sequence of length N and V is the voice activation factor.

From formula (1) we see that the effect of the so called CDMA *self-noise* can be reduced increasing the factor G_p (usually named *spreading factor*), and/or reducing the average quadratic cross-correlation coefficient μ_j^l .

In particular in approximated formula (1) we observe the self noise effect reducing with $\mu_j G_p^{-2}$. For Gold codes $\mu_j = 1$ and it can be shown a self noise reduction with respect to the asynchronous CDMA equal to G_p [6].

Furthermore, thanks to the system chip coherency, we can minimize for a given number of users the average quadratic cross-correlation factor μ_j^l , defined by eqn. (2) and characterizing the family of signature codes used.

The selection of code family for the proposed system is the trade-off result between the number of required quasi-orthogonal codes and their cross-correlation properties around the origin.

New code families matched to this particular application, having good cross-correlation properties around the origin and a larger size than Gold codes, are presently being investigated.

4.1 Numerical Results

System simulation is based on a time domain approach. The number of simultaneous users has been limited to 7 simply to limit the computation burden. The processing gain G_p has been consequently reduced to 15.5 to be representative of a large scale loaded CDMA system. The BER evaluation technique is based on the semi-analytical approach already used in a previous work [8].

It is easy to show that theoretical results for unfiltered S-CDMA system from [6], also apply to the case of BL-CDMA when the optimal receiver structure like the one drawn in Fig. 6 is used.

This theoretical result has been confirmed by simulation as shown in Fig. 7 where the theoretical BER for rectangular shaped chips (continuous line), is compared with simulations results (dots) obtained making use of Nyquist shaped chip pulses (roll-off factor $\alpha = 0.4$).

The previous results are in very good agreement with the theoretical calculation and Fig. 7 clearly shows the self-noise reduction achieved through system synchronization.

In order to assess the system robustness to the non linear characteristics of the high power amplifier, extensive simulations have been carried-out.

Fig. 8 also shows the simulated BER (cross) using a typical satellite L-band solid-state amplifier driven with 2.5 dB of output back-off. Minor BER degradation is observed around the nominal working point of 4 dB E_b/N_0 .

The results obtained are expected to be even better employing an higher processing gain.

Simulated BER sensitivity to the HPA output back-off at two different working points (dots and cross) is displayed in Fig. 8. Those results are slightly better than those already presented in [8] for the case of rectangular shaped chips (* and +).

Moreover the effect of the satellite HPA output filter has been analyzed by simulation. Using either an 8 poles Butterworth with two-sided bandwidth 1.5 the chip rate or an elliptical filter like the one described in section 3.1, no practical difference with the results of Fig. 8 has been observed.

Another point of major interest is the BER sensitivity to timing/frequency synchronization errors. To assess the impact of combined timing/frequency errors we have assumed an uniform frequency uncertainty of 100 Hz representative of

mobile motion and local oscillator instability, and we have derived the BER as a function of the maximum chip timing jitter. The calculation has been performed supposing uniform time jitter distribution and Gold codes signature sequences.

Fig. 9 compares theoretical (continuous line) and simulation results for rectangular chips (dots) with those obtained by simulation using two different roll-off factors (cross and stars).

In ref. [7] smooth BER dependence on frequency uncertainty range has been demonstrated.

5 Capacity Considerations

It can be shown that for the maximum number of users in the forward link ($[M_{CDMA}]_{fw}$) the following formula applies:

$$[M_{CDMA}]_{fw} \approx \frac{[\frac{N_0}{B_b}]_{req} - [\frac{N_0}{B_b}]_{ut} - X_{PIM}}{VR_b \left\{ \frac{L_d L_f K}{P_s G_s [\frac{G}{T}]_m} + \frac{S_{IM}}{(NPR)W_s} + \frac{\rho \alpha_f L_{nl}}{W_c} \left(\frac{\bar{\mu} R_b}{W_c} + \frac{1}{K_{rice}} \right) \right\}} \quad (3)$$

where:

L_d	: Path loss at the edge of satellite coverage.
L_{nl}	: Satellite transponder non linear amplifier loss.
L_f	: Average forward link fading loss.
ρ	: Polarization discrimination factor.
P_s	: Satellite available output power.
$[\frac{G}{T}]_m$: Mobile receiving antenna G/T .
G_s	: Satellite transmitting antenna gain.
α_f	: Satellite antenna discrimination factor.
K	: Boltzmann constant.
$[\frac{E_b}{N_0}]_{req}$: Required $\frac{E_b}{N_0}$ at the demodulator input.
$[\frac{E_b}{N_0}]_{ut}$: Uplink Hub to satellite $\frac{E_b}{N_0}$.
X_{PIM}	: Passive intermodulation noise factor.
R_b	: User bit rate.
S_{IM}	: Satellite amplifier intermodulation spreading factor.
NPR	: Satellite amplifier noise-to-power ratio.
$\bar{\mu} = \frac{1}{M} \sum_{i=1}^M \mu_i$: Global average quadratic cross-correlation factor.
W_c	: Spreading codes chip rate.
W_s	: Satellite channel bandwidth.
K_{rice}	: Rician fading factor.
V	: Voice activation factor.

More detailed description about the above parameters can be found in reference [4].

The return link formula is not shown because when including the return link propagation model it becomes of not trivial explanation, therefore out of the scope of the present work.

Observe in eqn. (3) that $\bar{\mu}$ (global quadratic cross-correlation factor), is in general dependent from $[M_{CDMA}]_{fw}$ hence eqn. (3) has to be solved with respect to the variable $[M_{CDMA}]_{fw}$. For particular code families like Gold it can be shown that $\bar{\mu} = 1$ hence eqn. (3) becomes of immediate application with an upper bound given by $N+2$ (Gold family size).

6 Conclusions

We have presented a satellite mobile communication system based on band limited quasi synchronous CDMA (BLQS-CDMA). Advantages of maintaining network synchronization

at chip level have been shown to consist in an easy mobile terminal synchronization even in presence of voice activation and shadowing together with CDMA self-noise reduction. This fact implies improved link transmission quality and, for the return link, reduced sensitivity to the near-far effect due to self-noise effect mitigation. Chip pulse shaping has been introduced to achieve signal band limiting. System performances have been verified through time domain computer simulation including channel non-linearity, filtering and imperfect timing and frequency synchronization. Finally a system capacity expression has been derived and its meaning and range of applicability discussed.

References

- [1] A. J. Viterbi, "Spread Spectrum Communications-Myths and realities," IEEE Communication Magazine, No.5 May 1979
- [2] M.B. Pursley, "Performance Evaluation for Phase-Coded Spread-Spectrum Multiple Access Communication-Part I and Part II," IEEE Transactions on Communications, VOL. 25, No. 8, August 1977.
- [3] I.M. Jacobs, K.S. Gilhousen, L.A. Weaver, K. Renshaw, T. Murphy, "Comparaison of CDMA and FDMA for the Mobilestar System," Proceedings of the International Mobile Satellite Conference, Pasadena California, May 3-5 1988
- [4] R. De Gaudenzi, C. Elia, R. Viola, "High Efficiency Voice Activated CDMA Mobile Communication System Based on Master Code Synchronization: System Analysis," ESA Working Paper 1543, September 1989.
- [5] R. De Gaudenzi, R. Viola, "Système de Communication à Access Multiple par Repartition à Codes avec Porteuse Activée par la Voix de l' Usager et Synchronisation par Code ESA Patent Filed in France, August 1989.
- [6] R. De Gaudenzi, R. Viola, "High Efficiency Voice Activated CDMA Mobile Communication System Based on Master Code Synchronization," In the proceedings of the IEEE Global Telecommunications Conference GLOBECOM, Dallas, Texas, November 27-30 1989.
- [7] R. De Gaudenzi, C. Elia, R. Viola, "Performance Evaluation of Quasi-Synchronous Code Division Multiple Access (QS-CDMA) for Satellite Mobile Systems," To be presented at the IEEE Global Telecommunications Conference GLOBECOM, San Diego (CA), December 2-5 1990.
- [8] R. De Gaudenzi, R. Viola, "A Novel Code Division Multiple Access System for High Capacity Mobile Communication Satellites," ESA Journal Vol.13, No. 4, December 1989.

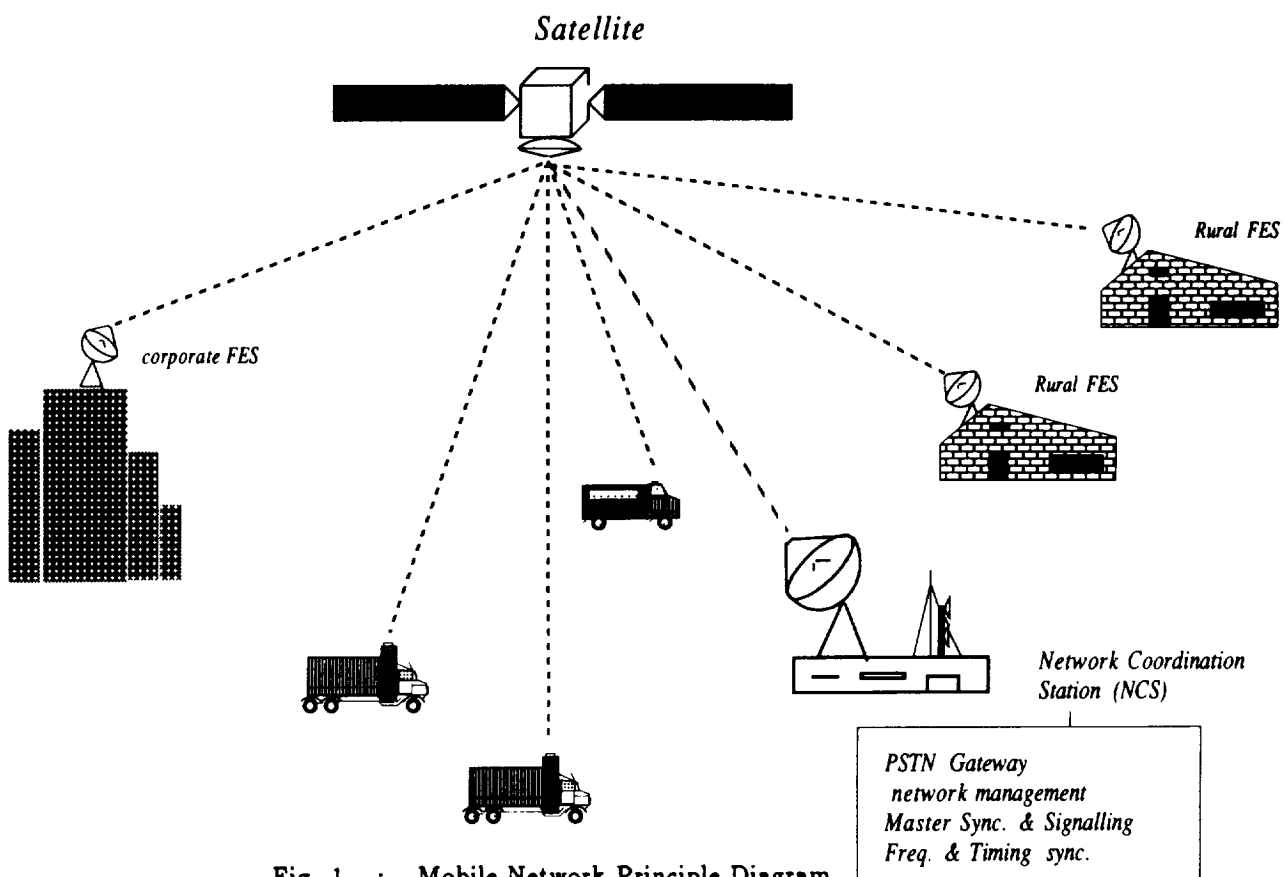


Fig. 1 : Mobile Network Principle Diagram

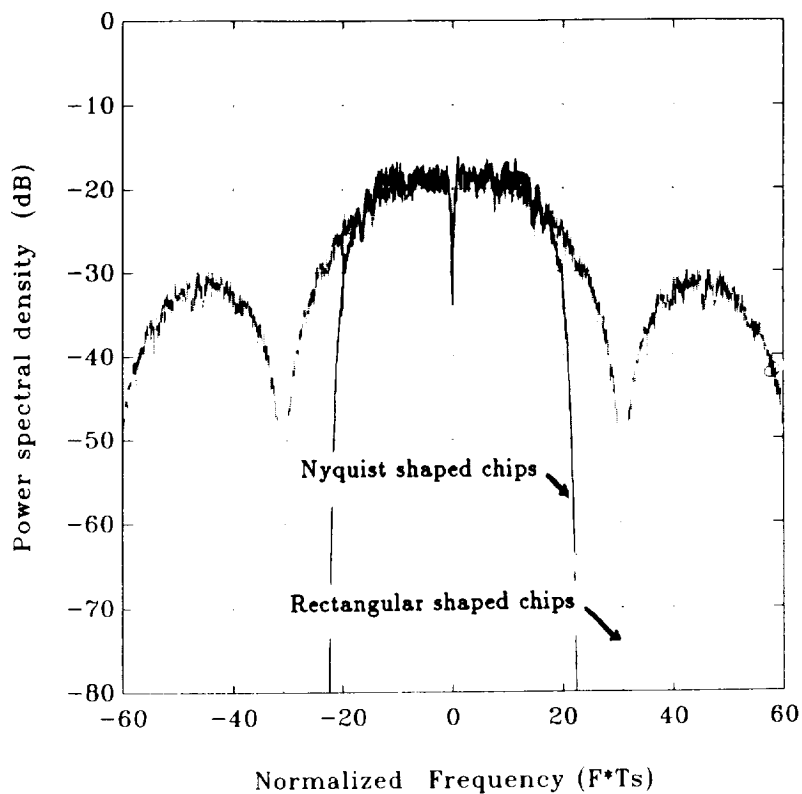


Fig. 2 : BLQS-CDMA spectrum: satellite input

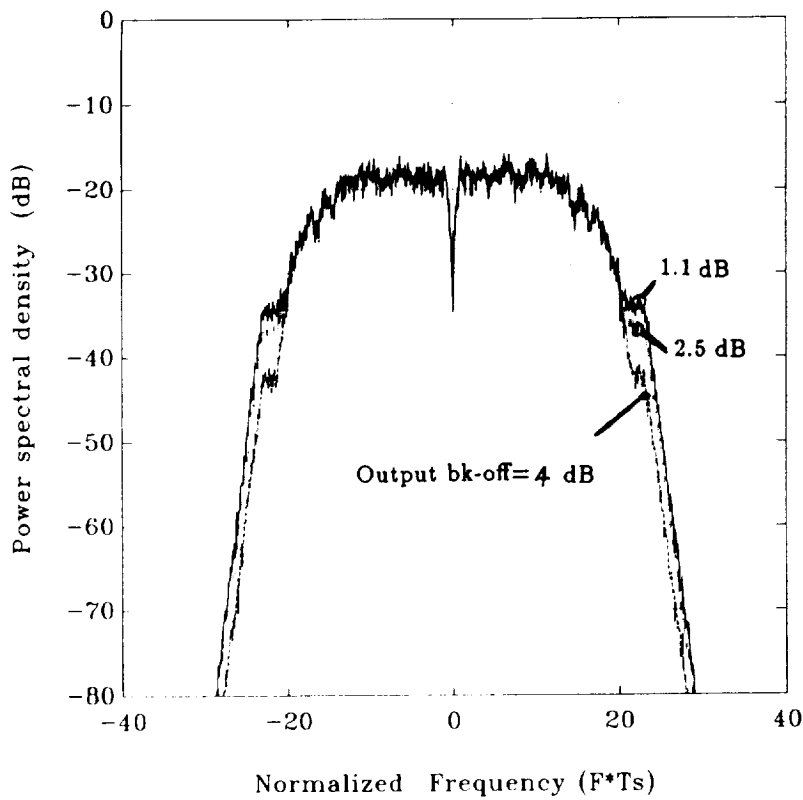


Fig. 3 :
BLQS-CDMA spectrum: satellite output

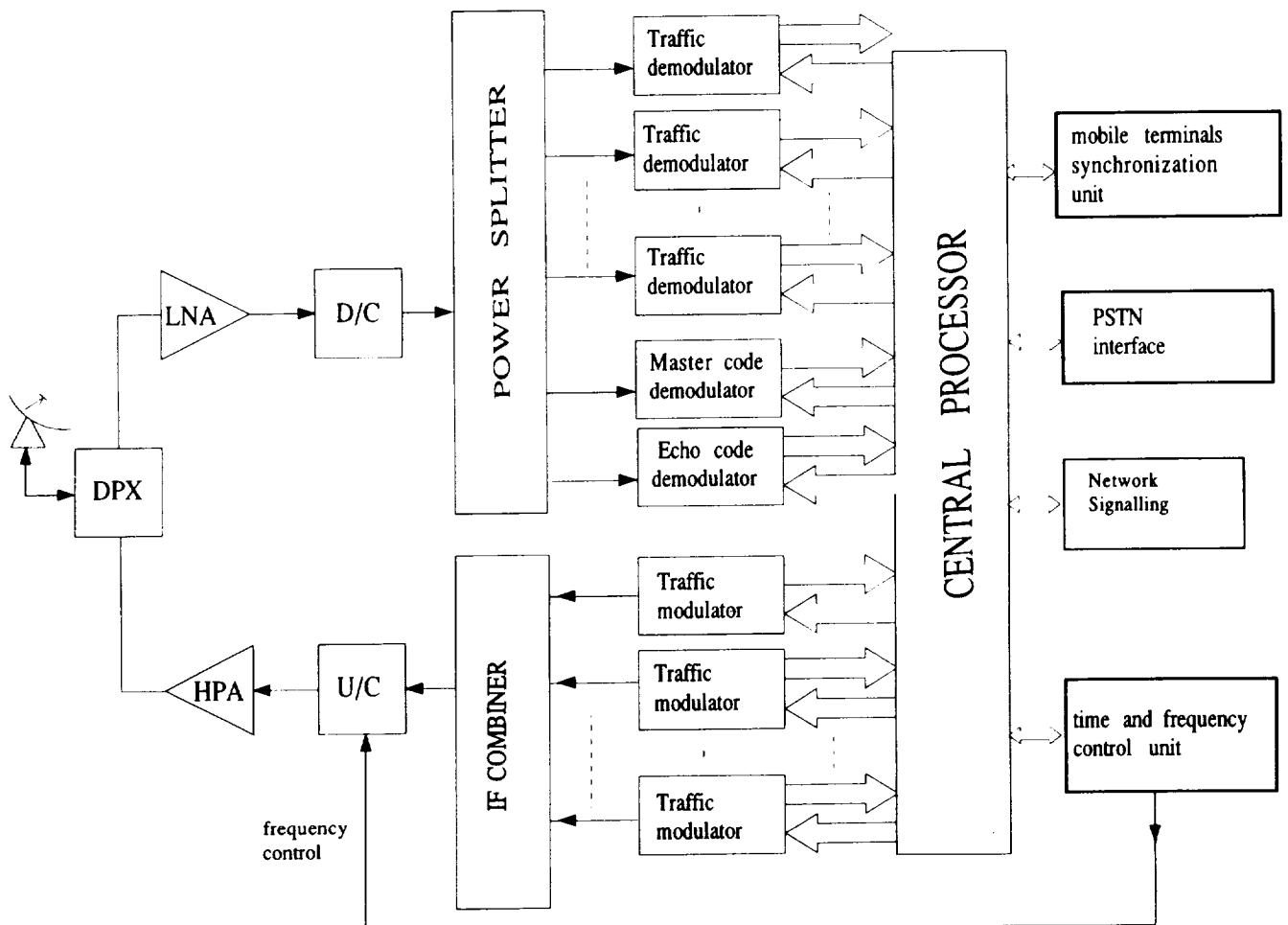


Fig. 4 : FES station block diagram

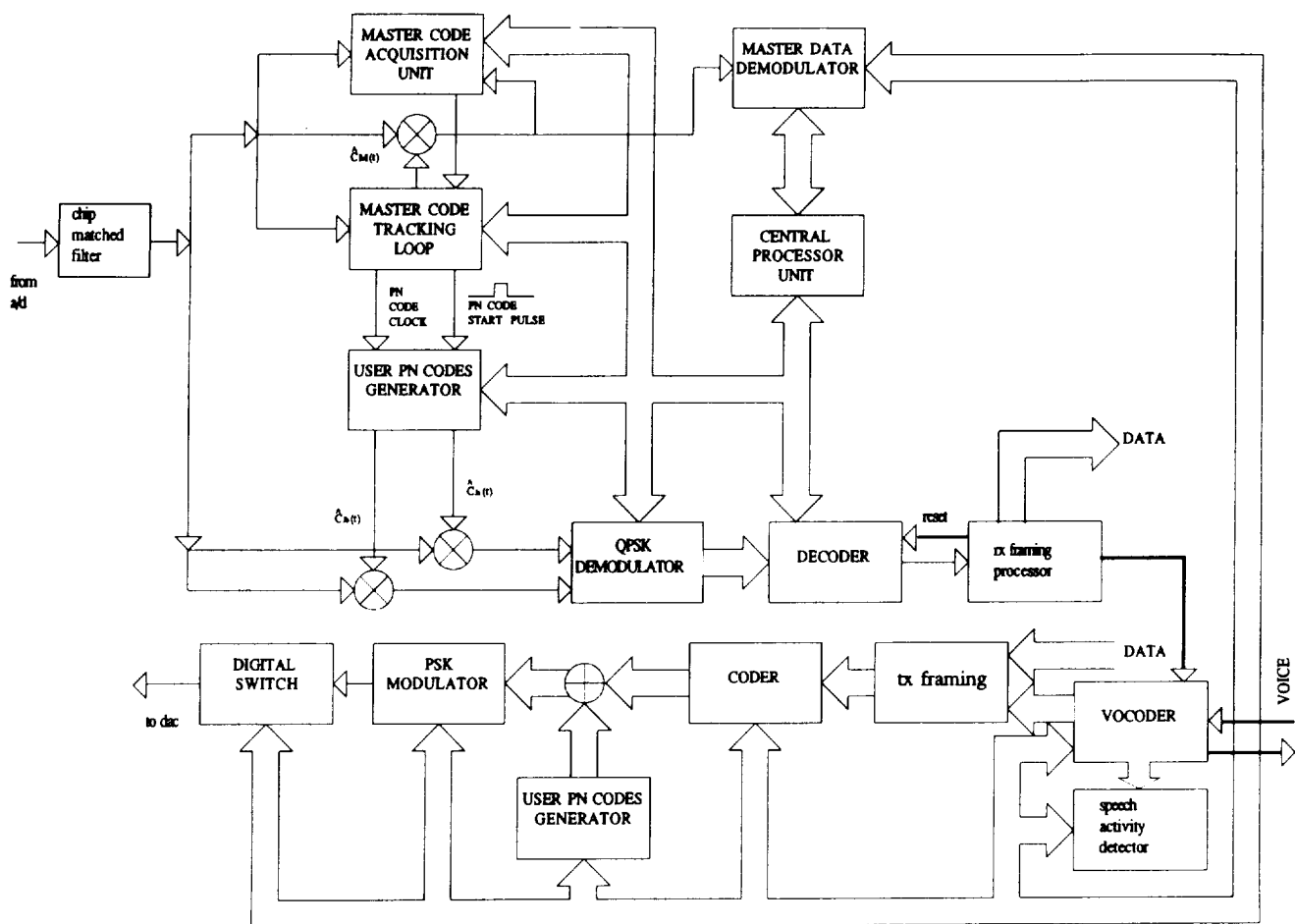


Fig. 5 : Mobile user terminal block diagram

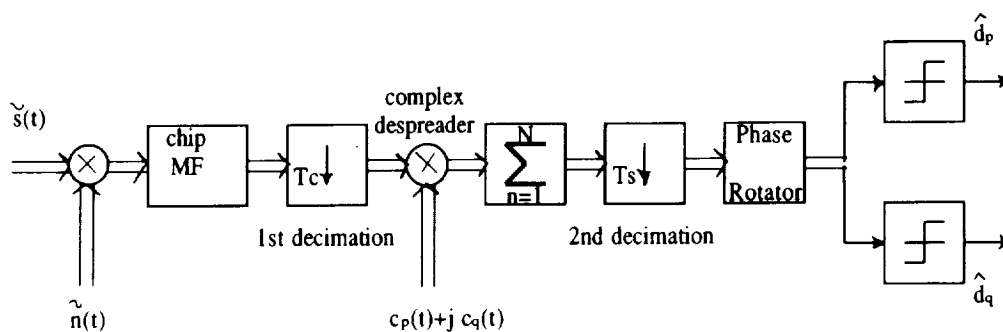


Fig. 6 : BLQS-CDMA demodulator block diagram

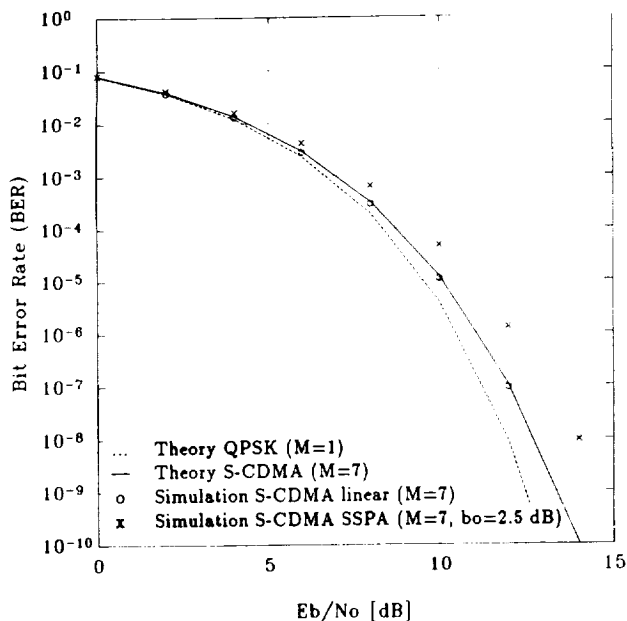


Fig. 7 : Probability of error vs. E_b/N_0 , $G_p = 15.5$, $M = 7$

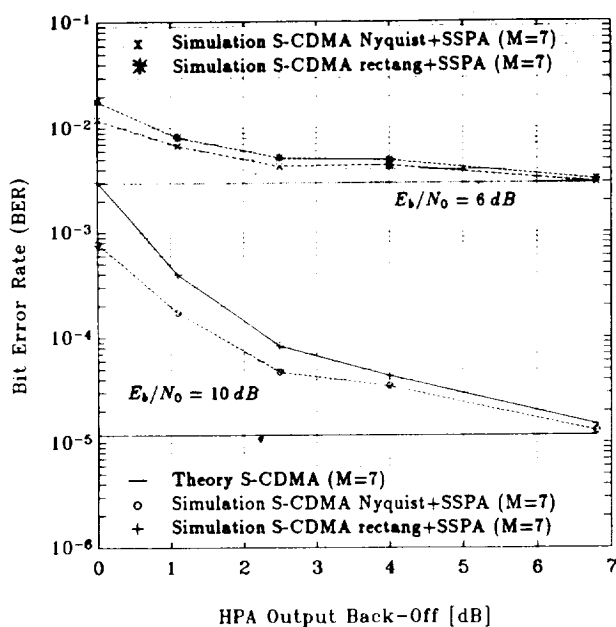


Fig. 8 : Probability of error vs. SSA back-off, $G_p=15.5$, $M = 7$

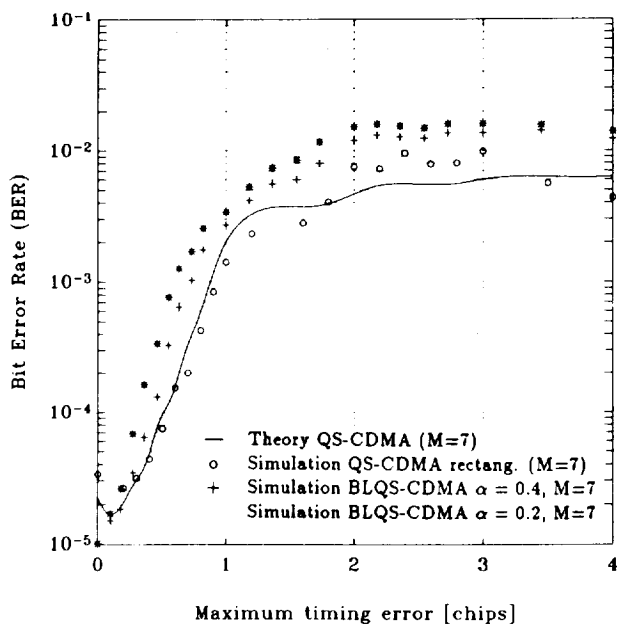


Fig. 9 : Probability of error sensitivity to timing jitter